DELPHI Collaboration

DELPHI 2004-037 CONF 712
July 29, 2004

A study of depletion of fragmentation particles at small angles in *b*-jets with the DELPHI detector at LEP

M. Battaglia[1], **R. Orava**[1,2], **L. Salmi**[2]

[1] Department of Physics, University of Helsinki, Finland

[2] Helsinki Institute of Physics, Finland

Abstract

Perturbative QCD predicts that gluon radiation off an energetic heavy quark is suppressed at small emission angles, resulting in the depletion of fragmentation particles around the direction of the primordial quark (dead cone effect). A search for this effect has been performed on data collected with the DELPHI detector at LEP at center-of-mass energy of 91.2 GeV. The decay vertices of b- and c-hadrons were reconstructed, and the particles not originating from the decay vertex were considered as fragmentation particles. To observe the depletion, the angular distributions of fragmentation particles in b- and c-jets were compared, with systematic checks performed also with light quark (u, d, s) jets.

Contributed Paper for ICHEP 2004 (Beijing)

1 Introduction

According to perturbative QCD there is a minimum angle for gluon emission off energetic heavy quarks[1]. As a consequence, a *dead cone* is formed around the original quark direction. Inside this cone there are few, if any, particles.

The limiting angle θ_0 for soft gluon emission is given by $\theta_0 = \frac{m_Q}{E_Q}$, where m_Q is the mass of the quark and E_Q its energy. For energetic light quarks the angular distribution is expected to be approximately proportional to $1/\theta$. In the case of heavy quarks, the existence of a minimum emission angle results in an angular distribution proportional to $\frac{\theta^3}{(\theta^2+\theta_0^2)^2}$ [2]. Thus the ratio of the two angular distributions is expected to be

$$\frac{\frac{dN_b}{d\theta}}{\frac{dN_{uds}}{d\theta}} \propto \frac{\theta^4}{(\theta^2+\theta_0^2)^2}, \tag{1}$$

or, in the case of b- and c-jets,

$$\frac{\frac{dN_b}{d\theta}}{\frac{dN_c}{d\theta}} \propto \frac{(\theta^2+\theta_{0,c}^2)^2}{(\theta^2+\theta_{0,b}^2)^2}. \tag{2}$$

These distributions are depicted in Figure 1. The theoretical ratios get very close to zero

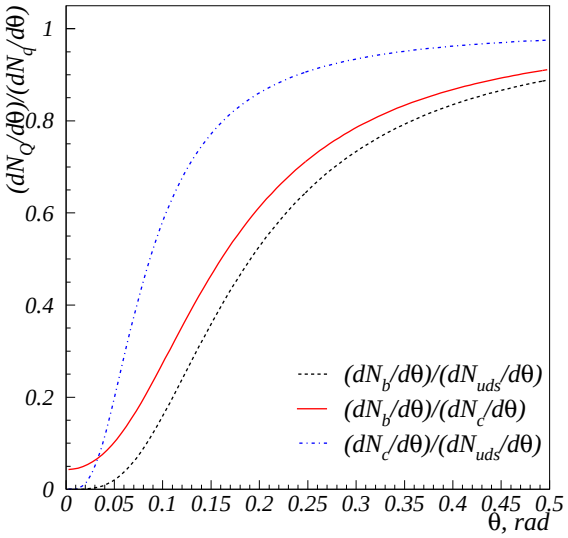

Figure 1: *The expected ratios of angular distributions of fragmentation particles when comparing b- and light quark jets (dashed line), b- and c-jets (solid line), and c- and light quark jets (dash-dotted line).*

at small angles when comparing with light quarks, due to the assumed $1/\theta$ behaviour of the distribution. However, at very small angles this assumption does not hold. It must also be noted that the experimental resolutions involved in the measurement of angular distributions of the fragmentation particles are such that the small angle region is expected to be filled somewhat.

So far the dead cone effect has not been observed directly, but indirect evidence of the effect has been provided by the measurement of the energy-independent multiplicity

differences in b and uds jets at DELPHI[3]. Flavour-independent fragmentation would have the multiplicity difference fall as the center-of-mass energy increases, whereas the observed energy-independence is consistent with the perturbative QCD predictions.

The main challenge in observing the dead cone effect is to separate the fragmentation particles from the decay products of the heavy quark. The decay products tend to populate the small-angle region left depopulated by the dead cone effect.

This study is based on a topological analysis of hadronic $Z^0 \to q\bar{q}$ decays recorded with the DELPHI detector at LEP. The analysis technique developed for this relies on tagging criteria based on particle topology and kinematics. These are used for the identification of the jet flavour and the separation of particles originating from the hadronization of the primordial quark and the decay products of that hadron (referred to as *decay particles* in the following) from those produced in the fragmentation process (referred to as *fragmentation particles*).

The dead cone effect is expected to be the largest when comparing angular distributions of fragmentation particles in b and light quark jets, as seen in Figure 1. However, in light quark jets the identification of the particle carrying the primordial quark cannot be performed as well as in the case of heavy quark jets, where the decay vertex of the heavy quark can be reconstructed. Therefore angular distributions in b- and c-jets are compared, and light quark jets are only used as a systematic check.

2 Event selection

This study is based on a sample of 2.1 million $e^+e^- \to Z^0 \to q\bar{q}$ events collected with the DELPHI detector in 1994 and 1995. Due to lower statistics, in the study of c jets also events collected in 1992 and 1993 were used, resulting in a total of 3.4 million hadronic Z^0 decays. A sample of simulated events equivalent to about 2.7 times the data has been used to study the efficiencies of separation between decay particles and fragmentation particles.

In order to avoid effects due to energetic gluon jets, two-jet events were selected by accepting only events with event thrust $T > 0.95$. The thrust was used in order to avoid a possible bias due to jet-finding algorithm. This criterion selected 1.9 million events in 94+95 data.

Samples of jets of different flavours were selected by using DELPHI b-tagging algorithm based on impact parameters of particle tracks[4].

The b jet sample was selected using the probability P_H for all the tracks in a single hemisphere to originate from the main event vertex. By requiring $P_H < 0.01$ a sample consisting of 81% b jets was obtained with an efficiency of 33% to select a b jet. For the analysis, the hemisphere opposite to the hemisphere used for event selection was used.

The sample of light quark jets was obtained by requiring that the probability P_E for all tracks in the event to originate from the main vertex satisfied $P_E > 0.3$. A vertex reconstruction was performed for the selected light quark jets, and in case a secondary decay vertex was reconstructed, the event was rejected. It was also explicitly required that the hemisphere used in the study contained at least two particles that satisfied the particle selection criteria. In the cases of b- and c-jets this requirement was implicit due to the requirement of at least two-particle decay vertex.

The c jet sample was obtained by selecting jets containing an exclusively reconstructed

Table 1: The angular resolutions

jet flavour	σ_θ (mrad)
b	20
c	20
uds	30

D meson decay. The number of b and light quark jets in the sample was reduced by using information on the energy and proper decay time of the D meson, as well as the event b-tagging probabilities with and without the particles associated with the vertex.

For all events, the direction of the primordial quark was estimated using the event thrust direction. A study on simulated events showed that a typical quark direction resolution between 20 and 30 mrad depending on the quark flavour was achieved. The resolutions are listed in Table 1.

Only charged particles with measured momentum between 0.5 GeV/c and 50 GeV/c and at least one associated hit in the Microvertex Detector were used.

3 Vertex reconstruction in b jets

In jets selected in the b jet sample, the fragmentation particles were separated from the decay products of the heavy quark by inclusive reconstruction of the heavy quark decay vertex. The vertex reconstruction was done in two steps: first a seed vertex was found using the most probable b decay products, and then the compatibility of the other charged particles in the hemisphere with the seed vertex was tested to form the final vertex.

For the seed vertex the most energetic particle in the hemisphere and those tracks that have the largest impact parameters normalised to their errors (*ips*) were used. Starting with the most energetic particle and the particle with the largest ips, particles were added to the vertex, and after each addition, the vertex was required to fill the following criteria:

1. Invariant mass of the vertex $m_{\rm rec} < 5.5$ GeV/c^2.
2. Change in vertex χ^2, $\Delta\chi^2 < 3$ for each added particle.
3. Distance from the main event vertex $\ell_{\rm rec}$ positive and $\ell_{\rm rec} < 2$ cm.

After the seed vertex was defined, all the remaining charged particles in the hemisphere were tested for compatibility both with the seed vertex and the main vertex of the event. Of the particles more compatible with the secondary vertex, the one that gave the smallest $\Delta\chi^2$ and filled the criteria listed above, was included in the vertex, after which the remaining particles were again tested for compatibility with both vertices. This was continued until all the remaining particles were more compatible with the main vertex. A vertex was successfully reconstructed in 112800 events in data. By requiring a reconstructed vertex, the purity of the b jet sample increased to 87%.

The number of particles associated with the secondary vertex as well as the mass distribution of the vertices is shown in Figure 2. The measured angular distributions of fragmentation particles (particles not associated with the vertex) and decay particles (particles included in the vertex) are shown in Figure 3.

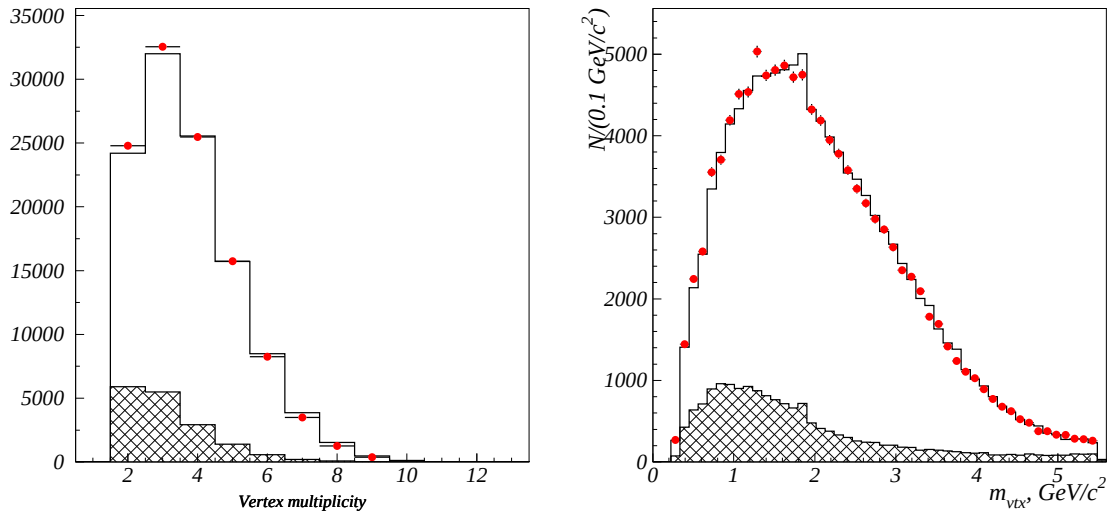

Figure 2: *The number of particles associated with the reconstructed vertex (left). The vertex mass distribution (right). Points are data, histograms simulation, the contribution of non-b-jets is shown hatched.*

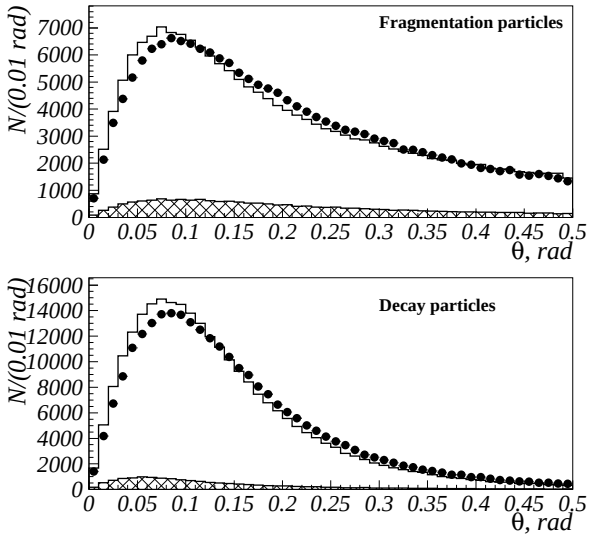

Figure 3: *The angular distribution of fragmentation particles (upper plot) and decay particles (lower plot) in the b jet sample. The hatched histograms show the contribution from c and light quark jets.*

4 Selection and analysis of c jets

Charm jets were identified by exclusively reconstructing the charm meson decay, and kinematical variables were used to separate genuine c jets from b jets that contain a charm meson from $b \to c$ decay.

The decay modes that were considered are

- $D^0 \to K^-\pi^+$
- $D^0 \to K^-\pi^+(\pi^0)$
- $D^+ \to K^-\pi^+\pi^+$ and
- $D^{*+} \to D^0\pi^+$, followed by
  - $D^0 \to K^-\pi^+$
  - $D^0 \to K^-\pi^+\pi^+\pi^-$
  - $D^0 \to K^-\pi^+(\pi^0)$
  - $D^0 \to K^0 e^+\nu_e$ or
  - $D^0 \to K^0\mu^+\nu_\mu$

and their charge conjugates. In case a decay was successfully reconstructed in both hemispheres, both hemispheres were also used in the analysis in order to increase the statistics. The details of the D decay reconstruction can be found in Ref [5].

In Figure 4 are shown the mass difference distribution for decays $D^{*+} \to (K^-\pi^+)\pi^+$ and mass distribution for $D^0 \to K^-\pi^+$ decays. The distributions contain a large contribution from background, mainly originating from b jets. If the mass m_D of the reconstructed

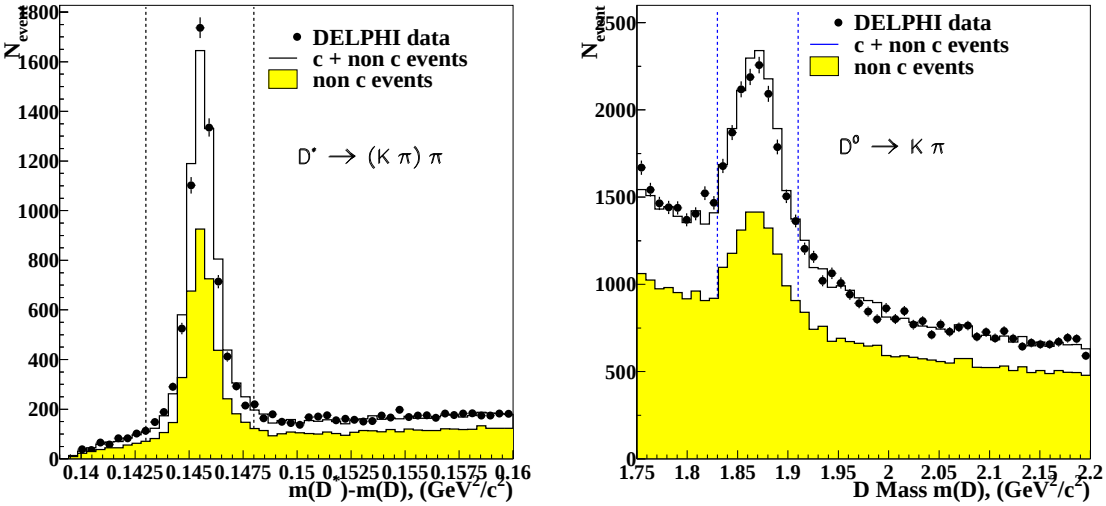

Figure 4: *Mass difference distribution for the decay channel $D^{*+} \to (K^-\pi^+)\pi^+$(left) and mass distribution for the decay $D^0 \to K^-\pi^+$ (right). The decays of D-mesons produced in B hadron decays can be seen among the background events, causing also background to peak in the signal region.*

D^0 or D^+, or the mass difference Δm was within the limits listed in Table 2, the event was accepted. The mass selection does not reduce the b-jet background considerably due to the fact that much of this background contains genuine D mesons produced in B decays. In order to improve the purity of the sample, further selection was done based on

Table 2: *The mass windows used to select the reconstructed D mesons.*

Decay mode	Δm (GeV/c^2)	m_D (GeV/c^2)
$D^{*+} \to (K^-\pi^+)\pi^+$	$0.143 - 0.148$	-
$D^{*+} \to (K^-\pi^+\pi^-\pi^+)\pi^+$	$0.143 - 0.148$	-
$D^{*+} \to (K^-\pi^+\gamma\gamma)\pi^+$	$0.141 - 0.151$	-
$D^{*+} \to (K^-\mu^+\nu)\pi^+$	< 0.180	-
$D^{*+} \to (K^-e^+\nu)\pi^+$	< 0.180	-
$D^{*+} \to (K^-\pi^+(\pi^0))\pi^+$	< 0.152	-
$D^+ \to K^-\pi^+\pi^+$	-	1.83-1.91
$D^0 \to K^-\pi^+$	-	1.80-1.93
$D^0 \to K^-\pi^+(\pi^0)$	-	1.50-1.70

1. Fraction of energy carried by the D meson, $X_E = E_D/E_{\rm beam}$
2. b-tagging probability P_E
3. Proper decay time of the D meson τ_D
4. b-tagging probability P'_E without the particles making the D meson.

Based on the shapes of the distributions of these variables in c-, b- and light quark jets containing a reconstructed D, the values of P_c, P_b and P_{uds}, corresponding to the likelihood of a jet to be a c, b or light quark jet, respectively, were computed. The distributions

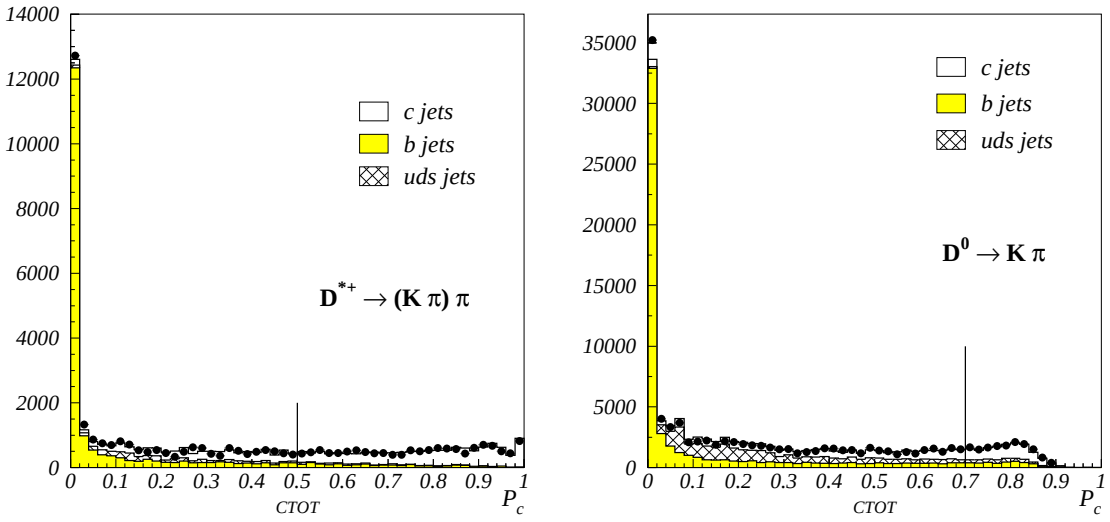

Figure 5: *Distribution of separation variable P_c for decay channels $D^{*+} \to (K^-\pi^+)\pi^+$ (left) and $D^0 \to K^-\pi^+$ (right). Points are data, histograms show the composition according to simulations. In the case of $D^{*+} \to (K^-\pi^+)\pi^+$, events with $P_c > 0.5$ were selected and in the case of $D^0 \to K^-\pi^+$, $P_c > 0.7$ was required.*

of P_c for the three types of jets for events with a reconstructed $D^{*+} \to (K^-\pi^+)\pi^+$ or $D^0 \to K^-\pi^+$ decay are shown in Figure 5. The selection values for each decay channel

Table 3: *The composition of each decay mode sample after selections based on the combined probabilities as well as the number of events selected in data.*

Decay mode	P_c	P_b	P_{uds}	c (%)	b (%)	uds (%)	events
$D^{*+} \to (K^-\pi^+)\pi^+$	> 0.5	-	-	84	13	3	1441
$D^{*+} \to (K^-\pi^+\pi^-\pi^+)\pi^+$	> 0.3	-	-	70	22	8	2135
$D^{*+} \to (K^-\pi^+\gamma\gamma)\pi^+$	-	< 0.3	< 0.4	74	19	7	1129
$D^{*+} \to (K^-\mu^+\nu)\pi^+$	> 0.4	-	-	72	22	6	1467
$D^{*+} \to (K^-e^+\nu)\pi^+$	> 0.35	< 0.7	-	65	25	10	1039
$D^{*+} \to (K^-\pi^+(\pi^0))\pi^+$	> 0.75	-	-	79	14	7	1315
$D^+ \to K^-\pi^+\pi^+$	> 0.8	-	-	74	24	2	1235
$D^0 \to K^-\pi^+$	> 0.7	-	-	62	22	15	2093
$D^0 \to K^-\pi^+(\pi^0)$	> 0.8	-	-	62	24	14	2424
All				70	21	9	14278

are tabulated in Table 3 together with the fractions of c, b and light quark jets in the sample, and total number of events accepted in data. The obtained c jet sample of 14278 jets consists, according to simulations, of 70% c jets, 21% of b jets and 9% of light quark jets.

Like in the case of b jets, particles not associated with the secondary vertex are considered fragmentation particles, and those in the vertex are considered decay products. Their angular distributions are shown in Figure 6.

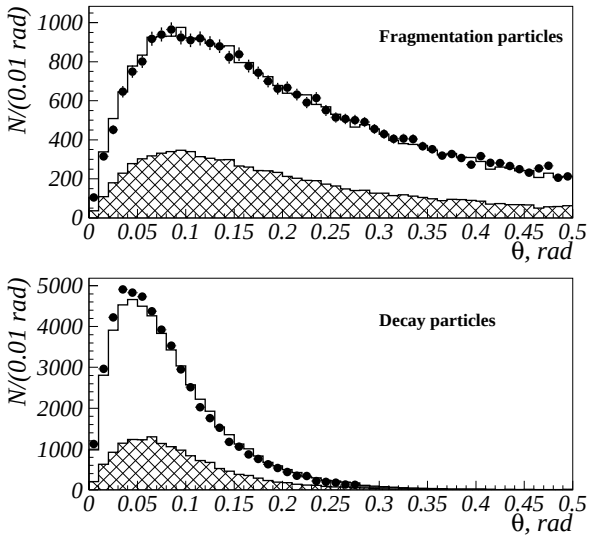

Figure 6: *The angular distribution of fragmentation particles (upper plot) and decay particles (lower plot) in the c jet sample. The hatched histograms show the contribution from b and light quark jets*

5 Light quark jets

In the case of light quark jets one cannot expect to be able to reconstruct the decay vertex of the particle carrying the primordial quark. However, this particle still needs to be removed from the sample in order to be able to compare light quark jets with b and $c$jets.

Particles satisfying any of the following criteria were considered as decay particles:

1. $p > 6.5$ GeV/c
2. $X_E = E_{\text{particle}}/E_{\text{hemi}} > 0.3$
3. Most energetic particle in hemisphere.
4. Identified as a K.

All the remaining particles were considered fragmentation particles. Using this selection, the obtained sample of fragmentation particles contained 76% of all fragmentation particles, and in the sample there was only 14% contamination from decay particles.

The angular distributions obtained for particles in light quark jets are shown in Figure 7.

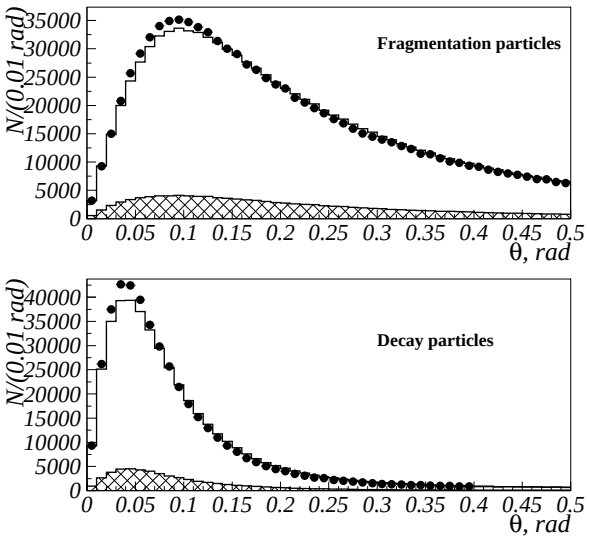

Figure 7: *The angular distribution of fragmentation particles (upper plot) and decay particles (lower plot) in the light quark jet sample. Hatched histograms show the contribution from b and c jets.*

6 Angular distribution analysis

First the remaining background was subtracted from the measured distributions. This was done by assuming that in each bin of the angular distribution the fraction of background is the same as it is in the corresponding bin of the simulated events.

Also the efficiency to correctly identify a fragmentation particles and decay particles varies as a function of the angle (Figure 8). While the behaviour of the efficiency to

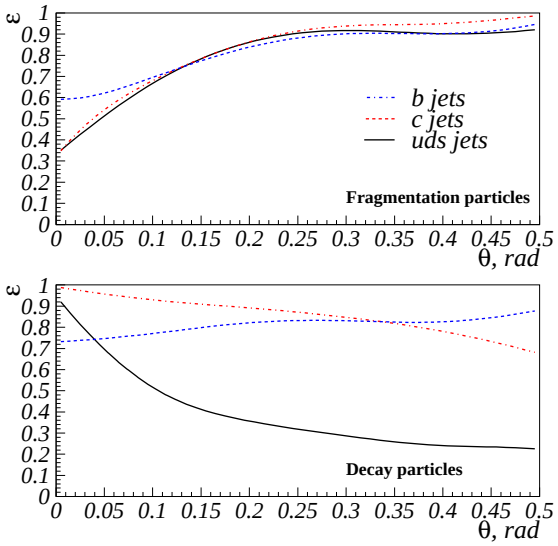

Figure 8: *The variation of the efficiency to correctly identify fragmentation particles (top) and decay particles (bottom) as a function of the angle in the three flavour samples.*

correctly identify fragmentation particles is similar for all the three jet types, the identification efficiency of decay particles in light quark jets drops rapidly when the angle of the particle with respect to the thrust direction increases. This is explained by the fact that the selection criteria for decay particles in light quark jets favour the selection of energetic particles, which also define the direction of the thrust.

It is necessary to correct the angular distributions for the variation of the efficiency. This was done using the efficiencies, obtained from simulations, ϵ_f^i and ϵ_d^i to correctly identify a fragmentation particle and decay particle, respectively, in bin i. Then the measured number of fragmentation particles is

$$n_f^{i,\mathrm{mes}} = \epsilon_f^i \cdot n_f^i + (1 - \epsilon_d^i) \cdot n_d^i, \tag{3}$$

where n_f^i and n_d^i are the true numbers of fragmentation and decay particles in that bin. Similarly, the measured number of decay particles is given by

$$n_d^{i,\mathrm{mes}} = \epsilon_d^i \cdot n_d^i + (1 - \epsilon_f^i) \cdot n_f^i. \tag{4}$$

Solving for n_f^i and n_d^i gives

$$n_f^i = \frac{\epsilon_d^i \cdot (n_f^{i,\mathrm{mes}} + n_d^{i,\mathrm{mes}}) - n_d^{i,\mathrm{mes}}}{\epsilon_f^i + \epsilon_d^i - 1} \tag{5}$$

and

$$n_d^i = \frac{\epsilon_f^i \cdot (n_f^{i,\mathrm{mes}} + n_d^{i,\mathrm{mes}}) - n_f^{i,\mathrm{mes}}}{\epsilon_f^i + \epsilon_d^i - 1}. \tag{6}$$

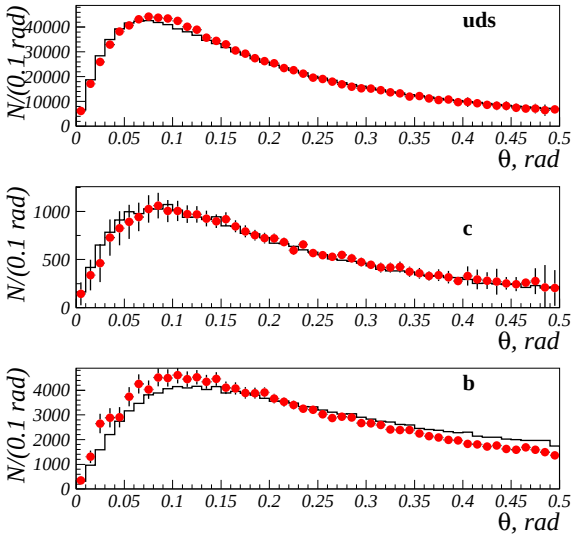

Figure 9: *The distributions of fragmentation particles after unfolding in light quark (top), c quark (middle) and b quark jets.*

The distributions of fragmentation particles after unfolding are shown in Figure 9.

Using simulated events the effect of event selection to the fragmentation particle distribution was studied, and it was found out that the efficiency is not constant over the angular range studied, and a correction was applied. Comparing the shapes of the cor-

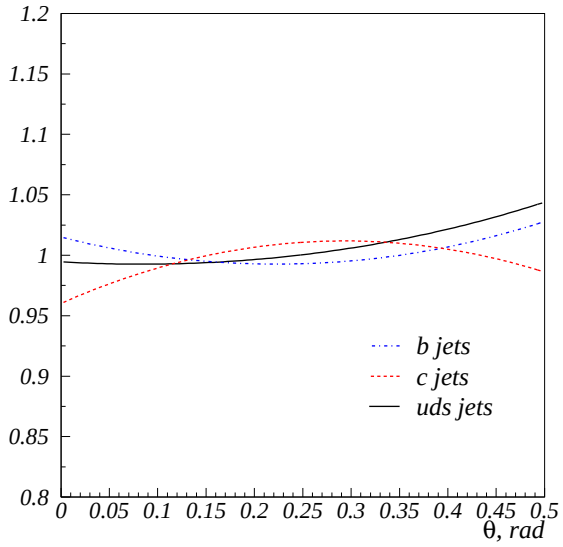

Figure 10: *The shapes of correction functions used to correct for the effect of event selection to the fragmentation particle distribution for b- (dashed), c- (dash-dotted) and light quark jets (solid line).*

rection functions (Figure 10), it can be noted that with respect to the uncorrected case, the corrected ratio of fragmentation particles in b and c events will show less depletion in the small angle region, since the correction in b jets gives more weight to events at small angles, and less weight in c jets.

7 Ratios of angular distributions

Since for b and c jets the separation of fragmentation particles and decay particles can be done by reconstructing the heavy quark decay vertex, it is a natural choice to compare the angular distributions of fragmentation particles in these two samples to study the possible depletion compatible with the dead cone effect.

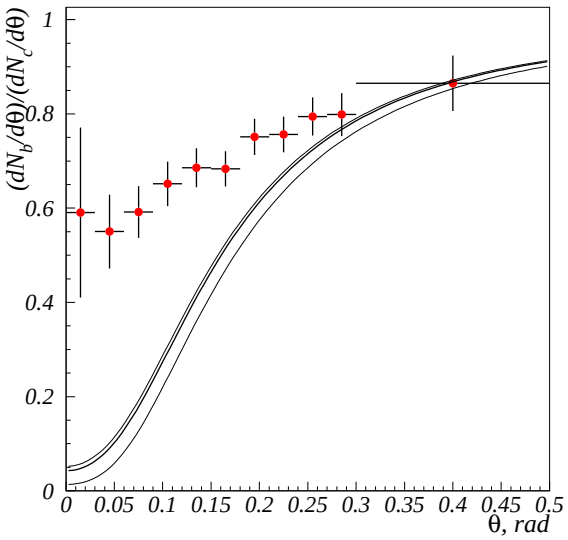

Figure 11: *The angular distribution of fragmentation particles in b jets divided by that in c jets. The thick solid line gives the theoretical expectation for the case of* $m_b = 4.2$ *GeV*$/c^2$, $m_c = 1.4$ *GeV*$/c^2$, $E_b = 34$ *GeV*, $E_c = 25$ *GeV, and the thinner lines correspond to* $m_c = 0.25m_b$ *and* $m_c = 0.35m_b$.

Figure 11 shows the ratio of the two angular distributions without any of the corrections applied to the angular distributions. Normalisation of the data was chosen such that the value in the bin extending from 0.3 rad to 0.5 rad coincides with the value of the function giving the theoretical behaviour in the center of the bin. The function was evaluated assuming $m_b = 4.2$ GeV$/c^2$, $m_c = 1.4$ GeV$/c^2$, and that the b and c quark carry 75% and 55% of the beam energy, respectively. Also shown are lines corresponding to $m_c = 0.35m_b$ and $m_c = 0.25m_b$ to illustrate the sensitivity of the function to changes in parameter values. The data shows relative depletion in b jets compared to c jets, as expected.

After applying the angular corrections shown in Figure 10, the distribution did not change significantly (Figure 12). In addition to statistical errors, systematical errors due to background subtraction, b fragmentation, B^{**} production, and purity of the c jets

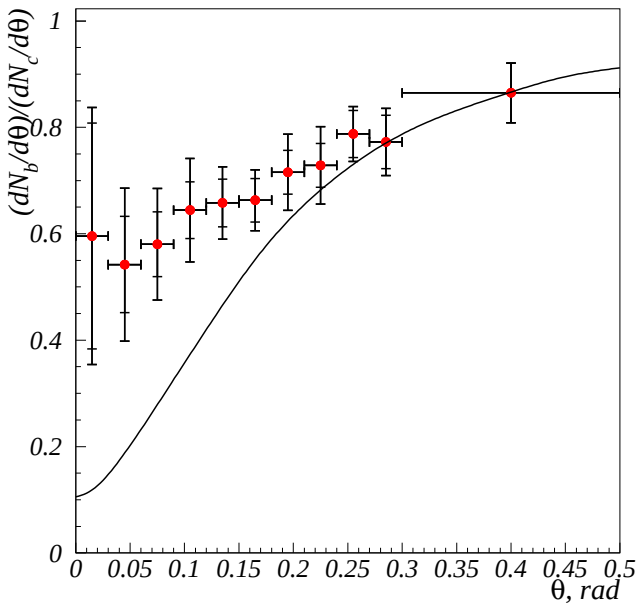

Figure 12: *The ratio of angular distribution of fragmentation particles in b jets and c jets. The systematic errors do not include the uncertainty coming from the definition of the angle. The solid line represents the expected behaviour folded with the angular resolution estimated from simulations.*

sample were evaluated. The effect of the angular resolution was not included in the systematic error. Instead, the expected angular distributions for b and c jets separately were folded with the respective resolutions estimated from simulations, and the ratio is shown as solid line in Figure 12.

To further study the effect of the angular resolution and the definition of the estimator for the primordial quark direction, the analysis was repeated with two alternative estimators, the direction of the jet the particle is associated with, and the direction of the reconstructed vertex. The latter definition was only available for b and c jets. The results for the ratio of angular distributions of fragmentation particles in b and c jets are shown in Figure 13, together with the expected distribution folded with the angular resolution estimated for the thrust direction. The normalisation region was extended to stretch from 0.24 to 0.5 mrad, since the statistical error in the normalisation bin was impractically large when using just the region from 0.3 to 0.5 mrad.

All different definitions of the primordial quark direction show depletion of fragmentation particles in b jets when compared with c jets. When the jet direction was used to define the quark direction the results are highly compatible with the results using the thrust direction, as was expected, since the event sample studied consisted mostly of two-jet events, where the thrust direction and jet direction more or less coincide. When the direction of the reconstructed vertex was used to define the quark direction, more depletion is seen than when using the other definitions for the quark direction, and the measured points follow reasonably well the expected shape. In principle, the vertex direction can be expected to be the most accurate estimator for the quark direction, but

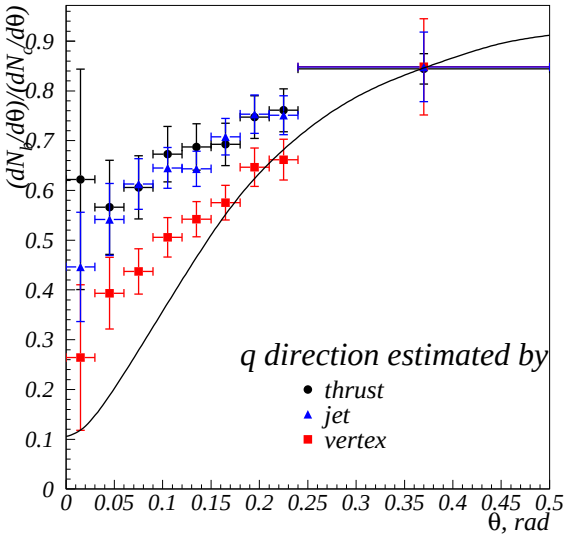

Figure 13: *The ratio of angular distribution of fragmentation particles in b jets and c jets, when the direction of the primordial quark has been estimated using the thrust direction (circles), jet direction (triangles) or the direction of the reconstructed vertex (squares). Also shown is the theoretically expected behaviour smeared with the angular resolution for thrust direction.*

on the other hand it suffers from the bias that fragmentation particles at small angles with respect to the vertex direction are very likely to be included in the vertex and thus to be classified as decay particles, especially in b jets, where the vertex is reconstructed inclusively. The exclusive c vertex reconstruction can be expected to suffer less from this. Also it needs to be noted that the statistical error in the normalisation bin is the largest when the vertex direction is used.

As a cross-check, the ratios of angular distributions in b and light quark and c and light quark jets were studied. The results are shown in Figure 14. Both ratios exhibit depletion in the small angle region, as expected.

8 Conclusions

The angular distributions of fragmentation particles in b-, c- and light quark jets were studied. The ratios of these distributions show depletion of particles at small angles with respect to the thrust direction in jets with heavy quarks, as expected from the dead cone effect.

Acknowledgements

We wish to thank V.A.Khoze for suggesting this topic and for being available to answer our questions.

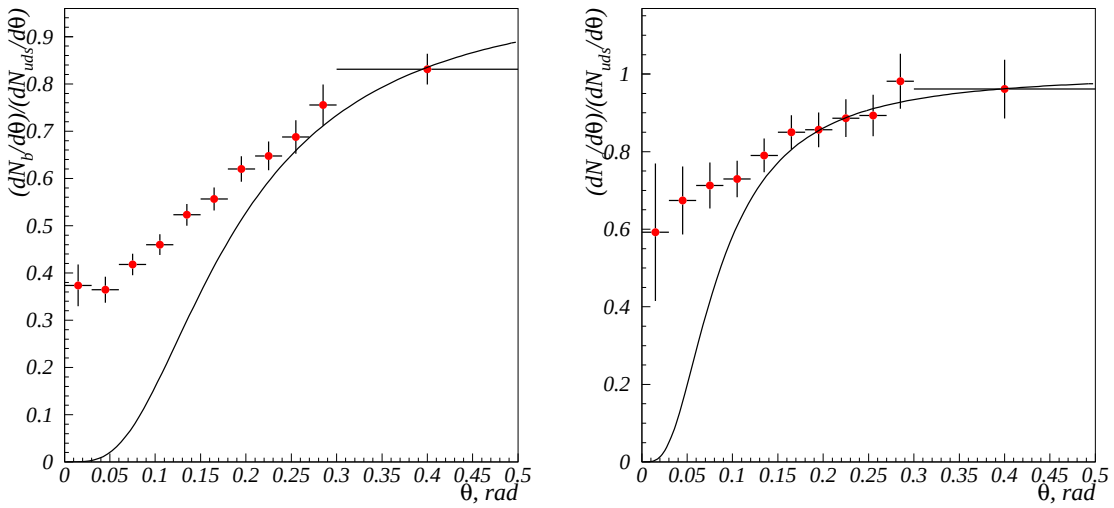

Figure 14: *The ratios of angular distribution of fragmentation particles in b jets and light quark jets (left), and the same for c- and light quark jets (right). The errors are statistical only. The functions show expected behaviour for* $m_b = 4.2$ *GeV*/c^2, $m_c = 1.4$ *GeV*/c^2, $m_{uds} = 0.01$ *GeV*/c^2, $E_b = 34$ *GeV*, $E_c = 25$ *GeV and* $E_{uds} = 16$ *GeV*.

References

[1] Yu.L.Dokshitzer, V.A.Khoze and S.I.Troyan, J.Phys. G17,1602(1991)

[2] V.A.Khoze, W.Ochs, J.Wosiek, Analytical QCD and multiparticle production, hep-ph/0009298

[3] P. Abreu *et al.* (DELPHI Collaboration) Phys. Lett.B479(2000)118

[4] J. Abdallah *et al.* (DELPHI Collaboration) Eur.Phys.J. C32 (2004) 185-208

[5] P. Abreu *et al.* (DELPHI Collaboration) Eur. Phys. J. C 10 (1999), 219